Effects of Zinc Occupancy on Human O^6-Alkylguanine−DNA Alkyltransferase†

Joseph J. Rasimas,‡,§ Sreenivas Kanugula,§ Paula M. Dalessio,‡ Ira J. Ropson,‡ Michael G. Fried,‡ and Anthony E. Pegg*,§

Department of Biochemistry and Molecular Biology and Department of Cellular and Molecular Physiology, The Pennsylvania State University College of Medicine, Hershey, Pennsylvania 17033

Received October 8, 2002; Revised Manuscript Received November 13, 2002

ABSTRACT: A recent crystallographic study of recombinant human O^6-alkylguanine−DNA alkyltransferase (hAGT) revealed a previously unknown zinc atom [Daniels et al., (2000) *EMBO J. 19*, 1719−1730]. The effects of zinc on the properties of hAGT are reported here. In bacterial expression systems, recombinant hAGT was produced in increasingly larger quantities when growth media are supplemented with up to 0.1 mM $ZnCl_2$. Metal-enriched hAGT samples had a 5-fold increase in repair rate constant over conventionally purified protein samples and a 60-fold increase over metal-stripped hAGT. In addition, mutants of the zinc-binding residues had decreases in zinc occupancy that correlated with reductions in repair rate. Zinc modulation did not abolish the repair capacity of a fraction of the hAGT population, as evidenced by the stoichiometric reaction with an oligodeoxyribonucleotide substrate. Zinc occupancy had a similar effect on the rate of reaction with O^6-benzylguanine, a free base substrate, as on the repair of methylated DNA. Differentially zinc-treated hAGTs showed the same affinity for binding to native DNA and substrate oligodeoxyribonucleotides. Metal content manipulations had little effect upon the CD spectrum of hAGT, but fluorescence studies revealed a small conformational change based upon metal binding, and zinc occupancy correlated with enhanced hAGT stability as evidenced by resistance to the denaturing effects of urea. These results indicate that the presence of zinc confers a mechanistic enhancement to repair activity that does not result from an increase in substrate binding affinity. Zinc also provides conformational stability to hAGT that may influence its regulation.

O^6-Alkylguanine−DNA alkyltransferase (AGT) is an important DNA repair protein that protects cells from the mutagenic, carcinogenic, and apoptopic events induced by a variety of endogenous and exogenous alkylating agents (reviewed in refs *1*−*5*). AGT is a small monomeric DNA repair protein whose homologues are found in a wide variety of prokaryotic and eukaryotic organisms. It is responsible for the repair of potentially mutagenic and cytotoxic alkyl and haloalkyl adducts of DNA, primarily at the O^6-position of guanine. Unlike many proteins that are responsible for maintenance of genomic integrity, AGT is not an enzyme, but instead, restores DNA by irreversible transfer of adduct substituents to an internal active-site sulfur atom [Cys145 in human AGT (hAGT)]. Two crystal structures of hAGT have recently been published, and while the overall structures reported are similar and both provide insight into the mechanism of this repair reaction, they differ on one specific aspect of the protein's structure. One model suggests the presence of a zinc atom bound within a coordination sphere of four amino acid residues (Cys5, Cys24, His29, and His85) near the N-terminus (*6*), while the other shows these residues in similar orientation but lacking the transition metal ion (*7*).

Until the incidental discovery of metal bound within crystals of hAGT, no prior experiments suggested that the hAGT might be a metalloprotein. AGTs from microbial and mammalian sources including hAGT have been studied quite extensively, and there is no evidence that a metal cofactor is needed for them to perform their DNA repair function, and none are present in their crystal structures of the *Escherichia coli* Ada C-terminal domain AGT (*8*) or the AGT from *Pyrococcus kodakaraensis* (*9*). In fact, transition metals have been viewed only as a potential source of interference with human hAGT function since various metals including Zn^{2+} as well as Cd^{2+}, Cu^{2+}, Hg^{2+}, and Ag^{2+} were found to inhibit activity (*10*, *11*).

There is, however, compelling evidence that zinc plays vital roles in other DNA repair processes. These include formamidopyrimidine−DNA glycosylase (*12*, *13*), the XP-A component of the nucleotide excision repair system that relies upon a zinc finger protein (*14*), and the N-terminal domain of Ada, which brings about methylphosphotriester repair and mediates the transcriptional activation leading to the adaptive response through the function of its larger N-terminal domain (*2*). In the latter case, autocatalytic activation of the nucleophilic cysteine residue that accepts the alkyl group by a tightly coordinated zinc ion is crucial to the protein's DNA repair function (*15*, *16*).

This mechanism is unlikely to apply to hAGT since the Cys145 acceptor site is not one of the residues complexed with zinc, and it was unclear whether the bound zinc found in the structure by Daniels et al. (*6*) is an experimental

† Supported by NIH Grants GM-48517 (M.G.F.), CA-18137 (A.E.P.), 5 T32 GM-08601 (J.J.R.), and 1 T32 ES-07312 (J.J.R.).

* Corresponding author. Tel: (717) 531-8152. Fax: (717) 531-7157. E-mail: aep1@psu.edu.

‡ Department of Biochemistry and Molecular Biology.

§ Department of Cellular and Molecular Physiology.

10.1021/bi026970b CCC: $25.00
Published on Web 01/10/2003

artifact, a normal but nonfunctional component of the protein structure, or plays a key functional role. We have therefore examined the structural and functional consequences of the relative zinc occupancy of the protein's putative zinc binding site. Assays for expression, activity, DNA binding affinity, and structural changes were performed while varying the protein's exposure to metal. Purified preparations of hAGT were handled meticulously to avoid unwanted metal contamination. Zinc content was modulated using equilibrium dialysis methods as described below without the addition of harsh redox reagents or chelators that might alter protein chemistry. Alterations of zinc occupancy at the specific metal binding site were achieved via site-directed mutagenesis of the four coordination sphere residues indicated by the crystal structure. Studies were also done using mutants of other cysteines, including the active-site Cys145 and a nearby residue Cys150. Our results indicate that hAGT is, indeed, a metalloprotein whose structural stability is enhanced by the presence of zinc in its N-terminal binding site. Furthermore, higher zinc occupancy is associated with more efficient rates of alkyl transfer by hAGT when using both methylated DNA and free base substrates. This enhancement in repair rates is independent of DNA binding and correlates with only minor perturbations in protein structure. The implications of these in vitro results and the potential significance of hAGT zinc occupancy in vivo are discussed.

MATERIALS AND METHODS

Materials. T_4 polynucleotide kinase was acquired from New England Biolabs. ATP[γ-^{32}P] was purchased from DuPont-New England Nuclear. Acrylamide, *N*,*N*′-methylene bisacrylamide, $ZnCl_2$, EDTA, and imidazole were purchased from Aldrich. Ultrapure urea was purchased from ICN Biomedicals, Inc. Dithiothreitol (DTT) and mineral oil were obtained from Sigma. All chemicals were reagent grade, unless otherwise denoted. A 16-residue oligodeoxyribonucleotide (5′-GACTGACTGACT**G**ACT-3′) and its compliment were purchased from Gibco-BRL. A substrate oligodeoxyribonucleotide with the same sequence and a methyl substitution at the O^6-position of the guanine in position 13 (shown in bold) was purchased from Synthegen LLC (Houston, TX)**.** Synthesis of substrate 16-mer oligodeoxyribonucleotide (5′-AACAGCCATAT**G**GCCC-3′) where the guanine shown in bold is methylated at the O^6-position was described previously (*17*). Samples of substrate oligo were repurified by HPLC, as required (*18*). O^6-Benzylguanine was generously provided by Dr. R. C. Moschel (ABL-Basic Research Program, National Cancer Institute−Frederick Cancer Research and Development Center, Frederick, MD). O^6-Benzyl[8-^{3}H]guanine (0.34 mCi/mmol) was prepared by catalytic tritium exchange of O^6-benzylguanine with tritiated water by Amersham Corp. and was purified as previously described (*19*). Samples of rat intestinal fatty-acid binding protein (IFABP) and spermidine/spermine N^1-acetyltransferase (SSAT) were available in our laboratory from published procedures (*20*, *21*).

AGT Proteins. Plasmids for expression of recombinant hAGT (wild-type and C145A mutant proteins) without $(His)_6$-tags from the pCX35 vectors (*22*) have been described. The construction of modified pQE-30 vectors encoding C-terminally $(His)_6$-tagged wild type, C145A, and C145S mutant hAGT proteins for expression in *E. coli* was accomplished using the pQE-30−AGT vector (*23*) as described (*24*).

The construction of $(His)_6$-tagged mutant proteins C5A, C24A, H29A, H85A, C62A, and C150A was accomplished by polymerase chain reaction with the modified pQE-30 vector as template and appropriate mutagenic primers using methods described previously (*25*). The primers not described previously (*25*) were as follows: 5′-CATCACGGATC-CATGGACAAGGAT**GCT**GAAATGAAACG-3′ (sense) for C5A, 5′-ACGTCCCCTTGCCCAGGAGCTTTATTTCGTGC-AGACCCTGCTC**ACG**ACCAG-ACAGCTC-3′ (antisense) for C24A, 5′-CCCCTTGCCCAGGAGCTTTATTTC**GGC**-CAGACCCTGCTCACAACC-3′ (antisense) for H29A, 5′-CCTGACGCGTGAACGACTCTTGCTGGAAAACGG-GATG**GGC**AAGCGCTGGCAC-3′ (antisense) for H85A, 5′-CCTGATGCAG**GCC**ACAGCCTGG-3′ (sense) and its antisense compliment for C62A, and 5′-CCGTGCCACA-GAGTGGTC**GCC**AGCAGCGGAGC-3′ (sense) for C150A. The entire coding sequence was checked to ensure that only the desired mutations introduced by the codons denoted in bold were present.

AGT Purification and Quantitation Assays. Recombinant wild-type and C145A hAGT proteins without $(His)_6$-tags were prepared as previously described using Polymin P precipitation, ammonium sulfate fractionation, and FPLC (*19*). His-tagged proteins were purified from cell lysates using TALON affinity resin (Clontech), in accordance with manufacturer's instructions and protocols previously detailed (*23*). Protein samples were homogeneous as judged by electrophoresis. Standard samples were dialyzed against 50 mM Tris buffer (pH 7.6) containing 5 mM DTT and stored frozen at −80 °C until needed. Zinc-supplemented samples were produced by dialyzing purified proteins against the above buffer containing 8 M urea and 100 μM $ZnCl_2$ (the solubility limit for zinc under these buffer conditions) for 24 h. Renaturation was accomplished by gradually decreasing the urea concentration in the dialysis buffer as follows: 12 h in 6 M urea, 12 h in 4 M urea, 12 h in 1 M urea, and 24 h in buffer without urea. Dialysis was carried out using 1 L of buffer for sample sizes of 0.1−0.5 mL at 4 °C with medium replacement every 6 h. Correct refolding was confirmed by circular dichroism (CD) analysis and assays of AGT activity (see below). Zinc-stripped samples were produced by dialyzing purified proteins against standard buffer with the addition of 8 M urea and 5 mM EDTA. EDTA was removed by equilibrium dialysis before the protein was allowed to refold by decreasing the urea concentration. Again, CD and activity assays were performed following refolding.

AGT concentrations were measured both by the BCA dye-binding assay (*26*) and spectrophotometrically using a molar extinction coefficient, $A_{280} = 3.93 \times 10^4\ M^{-1}\ cm^{-1}$, calculated from ref *27*. Values of $A_{215}/A_{280} = 8.2$ and $A_{260}/A_{280} = 0.63$ were obtained from UV spectra; extinction coefficients $A_{215} = 3.2 \times 10^5\ M^{-1}\ cm^{-1}$ and $A_{260} = 2.5 \times 10^4\ M^{-1}\ cm^{-1}$ were calculated from these ratios. Results of the two methods of protein estimation yielded concentrations, which agreed, in all cases, within 3% (results not shown).

Metal Content Determination. Glassware was washed extensively, and samples were handled with care so as to avoid introduction of exogenous metal ions. Metal content was determined by the highly sensitive method of inductively coupled plasma-mass spectrometry (ICP−MS) at Centre

Analytical Labs (State College, PA). Samples were analyzed for the following metals: Zn, Ni, Cd, Co, Cr, Cu, Fe, and Mg. In each case for standard, supplemented, and stripped samples, final dialysis buffers were used as blanks to allow for quantitation of metal-associated protein. From these measurements, binding stoichiometries were extracted by relating molar estimates of metal to molar estimates of protein concentration.

Imidazole Staining for Identification of Zinc Metalloprotein. A procedure was devised by adaptation of the technique relying on the ability of zinc ions to form insoluble precipitates with imidazole at acidic pH (*28*) to identify zinc metalloproteins resolved by gel electrophoresis. Purified protein samples were subjected to native polyacrylamide gel electrophoresis (PAGE), and the gel was subsequently incubated in 2 M imidazole adjusted to pH 5.0 with glacial acetic acid for 72 h at 21 °C. Formation of a white precipitate often occurs sparsely throughout the gel during the first 24 h, but later, following H_2O washes, it remains only in fixed bands corresponding to zinc metalloproteins. We have found that a densitometric scan of the gel superimposed upon a dark background followed by inversion of the image allows for the easiest visualization of white-stained protein bands.

Assays for hAGT Expression. Cultures of bacterial cell lines containing wild-type hAGT expression plasmids were grown in LB media supplemented with varying concentrations of $ZnCl_2$. Both XL-1 Blue cells containing a pQE plasmid for the expression of the C-terminal $(His)_6$-tagged protein and POP cells containing the pXC-35 native hAGT plasmid were tested for the effect of zinc levels in growth media on the expression level of the protein. Following appropriate growth and induction phases as previously described (*19*, *29*), 100 μL aliquots of each culture were removed and centrifuged at 22 000*g* for 1 min at 21 °C. Following removal of the supernatant, 20 μL of 0.125 M DTT was added to each pellet, and the samples were vortexed for 2 min. Samples were then heated to 90 °C for 5 min and subjected to PAGE in the presence of sodium dodecyl sulfate (SDS). Coomassie Blue staining was followed by densitometric quantitation of bands corresponding to the expression of recombinant hAGT. The level of expression for each set of growth medium conditions was calculated as a ratio of the hAGT band intensity corresponding to each sample to that from an uninduced culture using the same media.

A 5 mL aliquot of each of the cultures was used to generate crude protein lysates. Each culture was centrifuged at 5000*g* for 10 min at 21 °C, and the supernatant was decanted. To the pellet was added 200 μL of B-PER Lysis Buffer (Pierce). The mixture was vortexed and incubated on ice for 10 min. Following centrifugation at 22 000*g* for 10 min at 4 °C, the supernatant was collected, and from each of these lysates, 50 μg total protein was subjected to SDS−PAGE. Western blot analysis was performed as previously described using a polyclonal antibody directed against a region of the protein's N-terminus (*30*). Fluorometric analysis of band intensities served as a measure of protein expression for each sample corresponding to a given concentration of $ZnCl_2$ in the supporting bacterial growth medium.

Assay of Alkyltransferase Activity. The recombinant human protein and mutants C5A, C24A, H29A, and H85A were assayed for AGT activity essentially as described (*31*) using calf thymus DNA that had been methylated by reaction with *N*-[^{3}H]methyl-*N*-nitrosourea but omitting EDTA from all reaction buffers. $ZnCl_2$ was added to reaction mixtures at a concentration of 100 μM (the highest soluble concentration in Tris buffer at pH 7.6) where appropriate to test the effect of free zinc on AGT activity. Assay protocols were again followed as described, except for the omission of EDTA from reaction buffers or the appropriate addition of $ZnCl_2$ (*31*). Second-order rate constants for these repair reactions were calculated as previously described (*32*). Similarly, hAGT proteins were assayed for activity against the small molecule substrate O^6-benzylguanine. Proteins were incubated in various amounts with O^6-[8-^{3}H]benzylguanine in 50 mM Tris (pH 7.5) and 5 mM DTT in a volume of 0.25 mL, and time points were taken by halting reaction aliquots with buffer containing excess unlabeled substrate and guanine. Aliquots were separated by reverse-phase HPLC, and the eluate was monitored for radioactivity by mixing with 3.5 volumes of Flow Scint III and passing through a Radiomatic Flo-One Beta A A-140A radioactivity monitor. The rate constant was calculated as described (*33*). The C145A and C145S mutants lack the active-site acceptor residue and are therefore not active in alkyl transfer in either assay (*24*, *34*).

Determination of Repair Stoichiometry. hAGT proteins were assayed for their ability to dealkylate oligodeoxyribonucleotides containing O^6-methylguanine in accordance with the procedures previously outlined (*33*). Measured quantities of purified hAGT samples were incubated with 5′-d(AAC-AGCATATm^{6}GGCCC)-3′ in 50 mM Tris-HCl (pH 7.5) and 0.5 M DTT for 60 min. SDS was then added to 1%, and the mixture of oligodeoxyribonucleotides was separated by reverse-phase HPLC. Quantitative detection (A_{254}) of the alkylated substrate and unalkylated product oligodeoxyribonucleotide provided a measure of the total repair capacity of each of the hAGT proteins tested. As AGT brings about the stoichiometric transfer of alkyl adducts in an irreversible fashion, this assay serves as a measure of the fraction of repair-active AGT molecules within a given protein sample.

Electrophoretic Mobility Shift Assays (EMSA). A 16-residue oligodeoxyribonucleotide 5′-GACTGACTGACT-**G**ACT-3′ was used as a single-stranded ligand. Annealed with its complement (*31*), it was used in studies requiring double-stranded substrates. DNA samples were labeled with ^{32}P as described (*35*). DNA concentrations were measured spectrophotometrically, using $\epsilon_{260} = 1.3 \times 10^4$ M^{-1} cm^{-1} (per base pair) for duplex samples and $\epsilon_{260} = 1.04 \times 10^4$ M^{-1} cm^{-1} (per base) for single-stranded samples. Binding reactions were carried out in 10 mM Tris (pH 7.6), 1 mM DTT, and 10 μg/mL bovine serum albumin for 30 min at 21 ± 1 °C. Duplicate samples incubated for longer periods gave identical results, indicating that binding equilibrium had been attained. Samples were analyzed on native 10% polyacrylamide gels as described (*46*). Autoradiographs were obtained with Kodak X-Omat Blue XB-1 film, exposed at 4 °C. Gel segments containing individual electrophoretic species were excised using the developed film as a guide and counted in a scintillation counter by the Cerenkov method. Both the serial dilution (*36*) and the direct titration (*37*) methods were used to obtain data for the estimation of association constants (K_a). Association constants (K_a) were evaluated from the dependence of binding density (Y) on [hAGT] according to the following equation:

$$Y = \frac{[\text{hAGT}]^4}{\left(\frac{1}{K_a}\right) + [\text{hAGT}]^4}$$

Monomer-equivalent association constants are equal to the value of 1/[hAGT] at $Y = 0.5$.

Structural Analysis by CD. hAGT proteins were assayed for structural consequences of zinc occupancy by CD. A Jasco J-710 spectropolarimeter was used to probe for spectral changes in the far-UV (250−212 nm) using a thermostated 0.1-cm path length cell. Spectral measurements of 100 μg/mL protein samples in 20 mM sodium phosphate buffer (pH 7.6) were made in triplicate at both 25 and 37 °C.

Protein Stability Studies by Fluorescence. Unfolding experiments were done at equilibrium to determine the stability of the wild-type protein and single-site mutant proteins C5A, C24A, H29A, and H85A in the presence and absence of zinc. Denaturant stock solutions (10 M urea) used in unfolding experiments were prepared as previously described (*20*). A 9 M urea solution, containing the buffer components listed below, was prepared fresh from the frozen stock on the day of an experiment. All buffers contained 20 mM $NaPO_4$, 50 mM NaCl, and ±0.1 mM $ZnCl_2$, pH 7.6. Immediately before use, DTT was added to the buffer and urea solutions for a final concentration of 1 mM. Approximately 30 min before the start of an experiment, identical concentrations of protein were added to the buffer and 9 M urea solutions. Actual urea concentrations for all solutions were determined by refractive index with a Milton Roy Abbe-3 refractometer at 25 °C as previously described (*38*).

Equilibrium unfolding transitions as a function of denaturant concentrations were monitored by fluorescence with a PTI Quanta Master Luminescence Spectrometer in conjunction with a Hamilton Microlab 40C titrator. Initially, 2 mL of a buffer solution containing the native protein was placed in a 1 × 1 cm fluorescence cuvette containing a stir bar. This solution was overlaid with 200 μL of mineral oil to prevent losses in solution volume because of evaporation and to prevent the solutions from creeping up the walls of the cuvette. All titrations were carried out at constant volume and constant protein concentration using the titrator and the automated software provided for the instrument. One syringe of the titrator was used to withdraw an aliquot of the solution contained in the cuvette. The other syringe was used to add an equal volume of an identical concentration of protein in 9 M urea. The resulting solution was mixed and equilibrated for 10 min prior to collection of the fluorescence spectrum. The system was shown to be at equilibrium by obtaining identical results after doubling the equilibration times. This process of withdrawal of solution from the cuvette followed by addition of an equal volume of protein in denaturant gradually increased the concentration of urea in the cuvette. The urea concentration increment was calculated for each addition using the program Savuka (*39*). At least 45 cycles were done for each protein, increasing the urea concentration from 0 M to 7.5−8.5 M urea, depending on the volumes used for each cycle. The final urea concentration in the cuvette was determined using refractometry as described above. In all cases, the measured final urea concentration was less than 1% different from the calculated concentration.

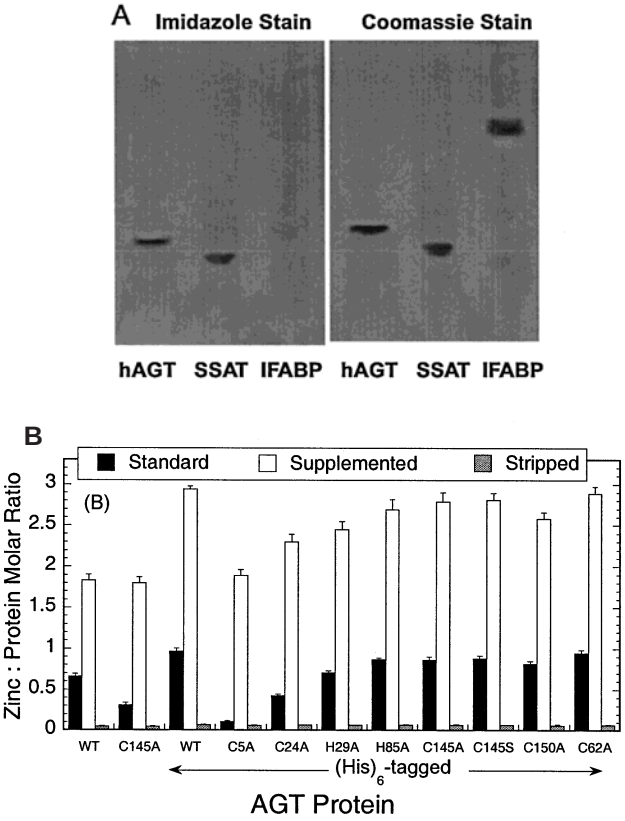

FIGURE 1: Qualitative and quantitative zinc analysis of hAGT samples. (A) Purified protein samples of hAGT, SSAT, and IFABP (10 μg each) were subjected to native PAGE, and the gel was subsequently stained for zinc by incubation in 2 M imidazole for 72 h at 21 °C as described in Materials and Methods. The standard Coomassie Blue staining is shown at the right and imidazole staining on the left. (B) ICP−MS was used to quantitate hAGT samples for zinc content. Wild-type hAGT and C145A were purified both with and without a C-terminal $(His)_6$ affinity tag; all other mutants shown are $(His)_6$-tagged. The first two columns correspond to nontagged proteins, and the remaining nine proteins have a purification tag. Standard, supplemented, and stripped samples were prepared and quantified as outlined in Materials and Methods. Binding stoichiometry is shown as the number of zinc atoms bound per molecule of protein.

The data were corrected for the background signal of the buffer and urea. Final protein concentrations ranged from 0.023 to 0.030 mg/mL, depending upon the protein used.

RESULTS

AGT Is a Zinc Metalloprotein. Because of the discrepancy between the two published crystal structures (*6*, *7*) and the lack of any prior evidence to the finding that hAGT is a metalloprotein, preliminary experiments were devised to confirm the presence of the potential zinc cofactor. As shown in Figure 1A, recombinant hAGT produced from the pXC-35 plasmid vector separated by PAGE stained strongly in a test for zinc proteins (*28*). IFABP, which has been extensively studied by a variety of structural methods and contains no metals (*40*−*43*), was used as a negative control and showed no staining (Figure 1A). These results clearly demonstrate that zinc is present and firmly attached in hAGT samples in significant quantities in accordance with the crystal structure reported by Daniels et al. (*6*).

ICP−MS was used to quantitate the metal content of hAGT preparations. In addition to being highly sensitive and

specific (*44*−*47*), this technique was not influenced by the presence of DTT, which may interfere with metal assays that rely upon chelating chromophores such as dithizone. The ICP−MS assay also allows for simultaneous analysis of multiple elemental species, but only zinc was present in significant quantities. Small amounts (less than a molar ratio of 1:20) of Fe, Mg, and Co were found (results not shown). The latter was presumed to originate from the TALON affinity resin (Clontech) used to purify $(His)_6$-tagged proteins, as it was only found in detectable amounts in those samples produced using this resin.

Zinc was present in much more substantial amounts than these metals in the recombinant hAGT proteins (Figure 1B). However, the recombinant hAGT preparations were not fully saturated with zinc as a substantial increase in zinc content was observed when the unfolded protein was renatured in the presence of excess zinc. Under these conditions, wild-type hAGT bound almost two zinc atoms per molecule of protein. The presence of a $(His)_6$-affinity tag further increased the binding stoichiometry by one additional metal ion (Figure 1B). SSAT, a protein that contains no zinc in its normal state, does have a bound zinc when a recombinant plasmid encoding the protein with a $(His)_6$-tag was used for production (Figure 1A). It is likely that one of the bound zinc atoms in the hAGT proteins purified using $(His)_6$ affinity tags was due to the association of the metal with the tag.

The ICP−MS measurements were consistent with the importance of key residues implicated in zinc binding by the crystal structure (*6*). Single alanine mutants were made of each of the four residues believed to comprise the N-terminal zinc coordination sphere of hAGT. Each of the residues appears to contribute to zinc binding, as the molar ratio of metal to protein is lower for each of the mutants as compared to wild-type hAGT for both standard sample preparation and after metal enhancement. Mutation of Cys5 resulted in the most significant decrease in zinc content as compared to wild-type hAGT, and C24A, H29A, and H85A show progressively less profound effects on zinc occupancy (Figure 1B). The C5A mutant clearly has one less bound zinc atom than wild-type hAGT, providing strong support for the structure identified by Daniels et al. (*6*).

The nature of the apparent third binding site is at present unclear. Mutations at Cys145 and at Cys150 had a modest effect on zinc occupancy (Figure 1B). It is therefore possible that despite their relatively inaccessible location in the active-site cleft, these residues can also bind zinc, particularly when the protein is exposed to a high concentration of the metal and other binding sites have been occupied.

Regardless of the presence of mutations or affinity tag, all hAGT proteins were effectively stripped of virtually all their bound zinc by treatment with EDTA and urea as described under Materials and Methods, effectively reducing the level of that ion to the range of all the other trace metals assessed by ICP−MS (Figure 1B).

Enhancement of Recombinant hAGT Expression by Zinc. Since purified recombinant hAGT samples have incomplete zinc occupancy, experiments were performed to investigate the effect of zinc-supplementation on the bacterial expression systems. *E. coli* cultures were grown and induced to generate wild-type hAGT in media containing various concentrations of $ZnCl_2$. Western blotting of cell-free extracts derived from the different cultures demonstrated enhancement in the expression of hAGT as the $ZnCl_2$ concentration was increased to 100 μM (Figure 2). Above that level of zinc, expression of hAGT decreased, possibly because of toxic effects of zinc on the growth of bacteria. Experiments of this type were performed using both POP cells containing the heat-shock inducible pXC-35 expression vector for hAGT and XL-1 Blue cells containing the pQE-30 expression vector for C-terminally $(His)_6$-tagged hAGT. Protein levels as measured by Western blotting varied consistently with $ZnCl_2$ concentration in each case (Figure 2). Data obtained from Coomassie Blue stained SDS−PAGE gels of whole-cell lysates from both of these expression systems gave similar results when the band corresponding to hAGT was quantified (not shown). Standard purified wild-type hAGT samples produced from culture media containing 100 μM $ZnCl_2$ had a molar ratio of zinc/protein of 0.80 ± 0.07:1, representing a slight enhancement over that for wild-type hAGT expressed from unsupplemented cultures which had a molar ratio of 0.66 ± 0.04:1. These results indicate that the availability of zinc during culture may influence hAGT protein expression and/or stability.

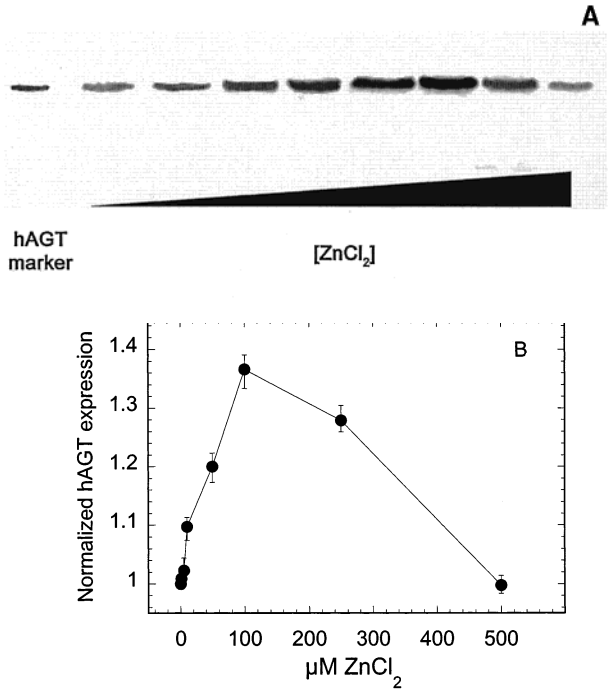

FIGURE 2: Effect of $ZnCl_2$ on recombinant human wild-type hAGT expression in *E. coli*. Panel A: $ZnCl_2$ content in culture media was varied over a range of 0−500 μM. Equal quantities (50 μg) of total protein from XL-1 Blue cell lysates were separated by SDS−PAGE and analyzed for hAGT expression by Western blotting. hAGT induction was quantitated by densitometric analysis of the band demarcated by the hAGT standard (leftmost lane). Panel B shows relative hAGT expression as a function of media $ZnCl_2$ concentration. Expression levels were normalized to that obtained with unsupplemented media. Error bars represent the standard deviation of six experiments—three using XL-1 Blue cells and three using POP cells.

Effect of Bound Zinc on Rate of DNA Repair. hAGT proteins were tested for DNA repair activity as a function of zinc occupancy. Second-order rate constants were determined for the alkyl transfer reaction with methylated DNA substrate by wild-type and mutant proteins (Figure 3A). In every instance, the repair rate correlated with the zinc content of the sample tested (cf. Figure 1A). A 5-fold enhancement

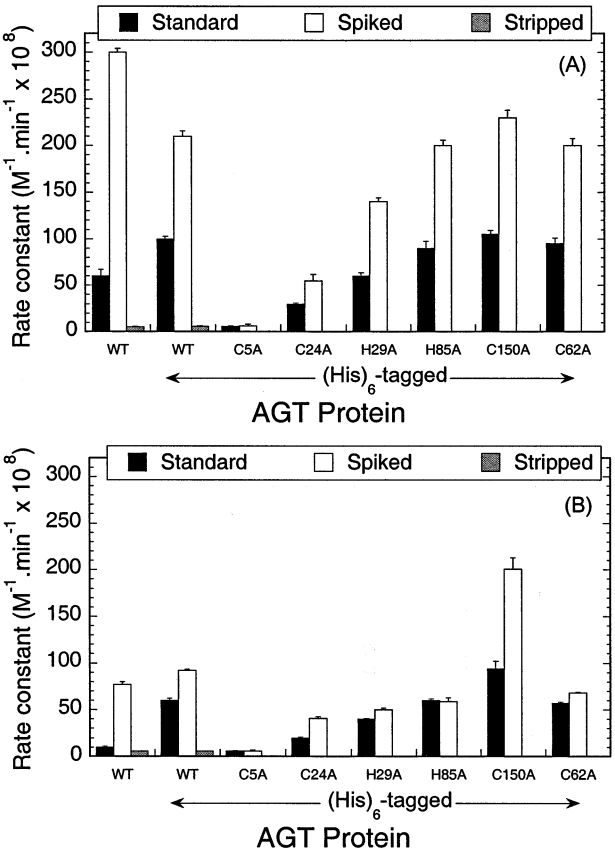

FIGURE 3: Effects of zinc content on DNA repair activity rate of hAGT. hAGT protein (3−60 ng) was incubated at 37 °C with 7 μg of [^{3}H]-methylated calf thymus DNA in 50 mM Tris (pH 7.5) and 5 mM DTT in a total volume of 1 mL. Time points were taken by halting reactions with buffer containing 8 M urea, and the rate constant was calculated as described in Materials and Methods. Studies with zinc-stripped samples were carried out only with wild-type hAGT preparations. Assays were performed in the absence (panel A) and presence (panel B) of 0.1 mM $ZnCl_2$.

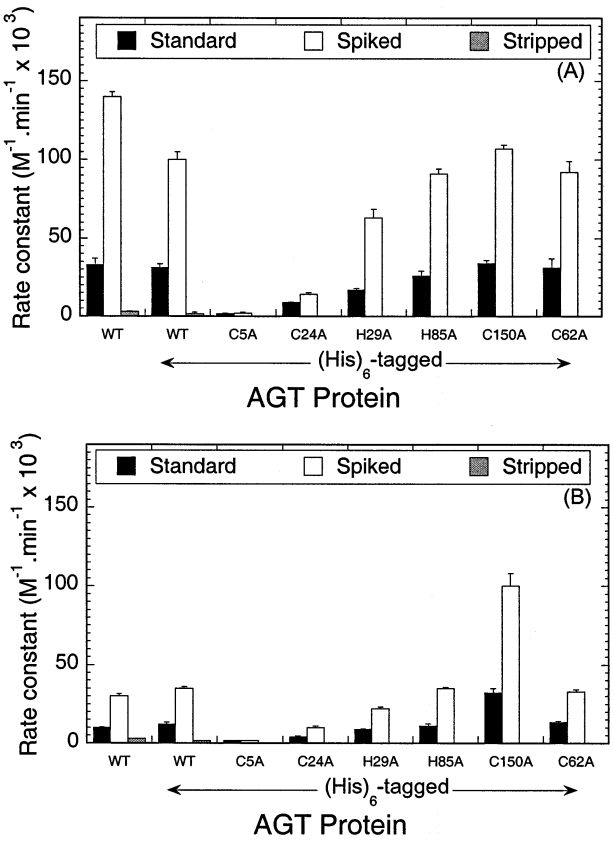

FIGURE 4: Effects of zinc content on the reaction of hAGT with O^6-benzylguanine. Proteins were incubated in various amounts with O^6-[8-^{3}H]benzylguanine in 50 mM Tris (pH 7.5) and 5 mM DTT in a volume of 0.25 mL, and time points were taken by halting reaction aliquots with buffer containing excess unlabeled substrate and guanine. Aliquots were analyzed for guanine formation, and the rate constant was calculated as described in Materials and Methods. Studies with zinc-stripped samples were carried out only with wild-type hAGT preparations. Assays were performed in the absence (panel A) and presence (panel B) of 0.1 mM $ZnCl_2$.

in repair rate was observed for the zinc-supplemented wild-type hAGT over that for standard preparations. Stripping the protein of zinc resulted in a 10-fold decrease in the rate constant as compared to standard wild-type hAGT. Furthermore, the $(His)_6$-tagged mutant hAGTs repaired DNA substrate less efficiently than similarly prepared $(His)_6$-tagged wild-type hAGT, with lower zinc occupancy yielding slower rates of repair in each case. These findings suggest that the presence of zinc bound within the N-terminal structure of hAGT influences the alkyl transfer reaction with DNA despite the lack of proximity of the metal to the C-terminal active site and DNA-binding motifs (*6*).

Activity assays were also performed for the same hAGT proteins in the presence of a high $ZnCl_2$ concentration to examine the effect of solution zinc on the DNA repair reaction. In agreement with previous reports of the inhibition of AGT activity by metals (*10*, *11*), rate constants in every case except C150A were decreased with 0.1 mM $ZnCl_2$ added to reaction mixtures (Figure 3B). Despite the inhibition of wild-type hAGT and the mutants by free zinc, however, the trend of repair efficiency increasing with AGT zinc occupancy remained.

Within experimental error, the repair rate constants for mutants C62A and C150A are identical to those of wild-type hAGT in standard and zinc-supplemented preparations (Figure 3). However, although the C62A protein was inhibited by $ZnCl_2$ to the same degree as wild-type hAGT, the rate constant was only slightly slower for C150A in the presence of zinc as compared to zinc-free assay conditions. Thus, the binding of zinc to Cys150, which is close to the active-site Cys145, may be related to zinc-mediated inhibition.

Effect of Bound Zinc on Rate of Reaction with O^6-Benzylguanine. The free base, O^6-benzylguanine, is a substrate for hAGT that transfers the benzyl group to Cys145 (*19*). Second-order rate constants for debenzoylation of this base are presented graphically in Figure 4. Although, as previously reported (*33*), the overall rates of repair were significantly slower than with methylated DNA substrates, the trends observed with respect to zinc occupancy were similar. Reaction with O^6-benzylguanine proceeds more rapidly when catalyzed by hAGT samples with higher zinc occupancy whether zinc levels had been modulated by preparation methods and/or mutation. This increase in repair efficiency as a function of hAGT zinc content suggests that the enhancement is mediated through an effect on the alkyl transfer reaction itself rather than upon other factors in AGT repair function such as DNA binding. In parallel experiments with 0.1 mM $ZnCl_2$ added to reaction mixtures, the effects were, again, similar to those observed with methylated DNA

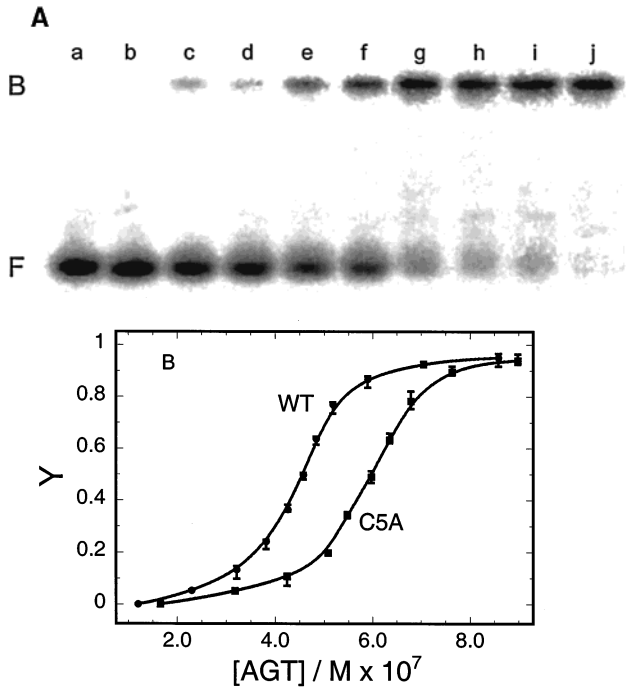

FIGURE 5: EMSA analysis of hAGT binding to DNA. Panel A: Binding to a double-stranded 16-mer was carried out at 21 ± 1 °C in 10 mM Tris (pH 7.6), 1 mM DTT, and 10 μg/mL bovine serum albumin. All samples contained 8.75×10^{-7} M DNA; samples in lanes a−j contained increasing concentrations of conventionally purified $(His)_6$-tagged C5A hAGT. Electrophoresis was performed as described in Materials and Methods. Bound DNA (B) and free DNA (F) are indicated. Panel B shows binding isotherms based upon the gel data shown in panel A and gel data from a similar experiment using conventionally purified $(His)_6$-tagged wild-type hAGT. Association constants are shown in Table 2.

(Figure 4B). The presence of free zinc resulted in decreased rates of reaction with O^6-benzylguanine for all hAGT proteins assayed except C150A, but the dependence of debenzoylation rate upon zinc occupancy was preserved. These results with a small molecule substrate in the absence of DNA suggest that free zinc in solution does not inhibit the alkyl transfer reaction by simply interfering with AGT−DNA binding.

DNA Binding Is Unaffected by Changes in Zinc Saturation. EMSA were performed to determine whether the observed changes in DNA repair rate reflect changes in binding affinity for DNA (Figure 5). The DNA used as ligand was the double-stranded 16-mer 5′-GACTGACTGACTGACT-3′. Previous studies have shown that hAGT forms 4:1 complexes with this oligonucleotide (*37*); none of the protein modifications employed to alter zinc occupancy changed that stoichiometry (J. J. Rasimas, unpublished observations). Association constants (K_a) evaluated from the dependence of binding density (Y) on [hAGT] are presented in Tables1 and 2. Although the different proteins displayed small variations in affinity (differences ≤3-fold), changes in zinc occupancy did not significantly affect affinity of hAGT for oligodeoxyribonucleotides not containing an O^6-methylguanine adduct (Table 1). Similar studies with single-stranded oligonucleotides (not shown) demonstrated a comparably small variation in binding constants. Association constants for active AGTs cannot be measured with substrates containing O^6-methylguanine because of the rapidity of the DNA repair reaction. However, repair-deficient C145A and C145S mutants provide adequate surrogates (*31*). The binding of these hAGTs with single- or double-stranded oligodeoxyribonucleotides containing O^6-alkylguanine residues were also unaffected by zinc occupancy (Table 2). The absence of a significant effect of zinc on DNA binding is consistent with binding models in which the zinc site is separate from the DNA binding domain.

Parallel experiments in which $ZnCl_2$ was added to binding reactions at a concentration of 0.1 mM returned K_a values that were not significantly different from those obtained in the absence of free metal ions (results not shown). This outcome is intriguing in view of the inhibitory effect of exogenous zinc on DNA repair. In crystal structures of hAGT, the side chain of Cys150 is located close to the active

Table 1: Binding of Zinc-Modulated hAGT Proteins to DNA[a]

	Monomer-Equivalent Formation Constants[b] × 10^{-6} M		
	Protein Preparation		
AGT protein	standard	zinc-supplemented	zinc-stripped
wild-type hAGT	1.00 ± 0.05	1.11 ± 0.06	1.00 ± 0.02
C145A hAGT	0.83 ± 0.05	0.91 ± 0.06	0.83 ± 0.04
$(His)_6$-tagged wild-type hAGT	2.17 ± 0.23	1.82 ± 0.22	2.50 ± 0.27
$(His)_6$-tagged C5A	1.67 ± 0.13	1.43 ± 0.05	
$(His)_6$-tagged C24A	1.7 ± 0.16	1.82 ± 0.15	
$(His)_6$-tagged H29A	2.13 ± 0.24	1.90 ± 0.17	
$(His)_6$-tagged H85A	1.54 ± 0.11	1.65 ± 0.06	
$(His)_6$-tagged C145A	1.81 ± 0.28	1.43 ± 0.09	1.66 ± 0.12
$(His)_6$-tagged C145S	2.91 ± 0.38	2.65 ± 0.23	2.65 ± 0.10

[a] Equilibrium binding reactions were carried out in 10 mM Tris (pH 7.6), 1 mM DTT, and 10 μg/mL bovine serum albumin at 21°C for 30 min. [b] Monomer-equivalent formation constants, equal 1/[hAGT] at half-saturation of the 4:1 complex of hAGT with double-stranded 16-mer oligodeoxyribonucleotide. Error ranges represent the standard deviation for three replicate experiments.

Table 2: Binding of Zinc-Modulated hAGT Proteins to DNA Containing O^6-Methylguanine[a]

	Monomer-Equivalent Formation Constants[b] × 10^{-6} M		
	Protein Preparation		
AGT protein and DNA	standard	zinc-supplemented	zinc-stripped
C145A hAGT + O^6-MeG ssDNA	2.08 ± 0.09	1.96 ± 0.13	2.04 ± 0.1
C145A hAGT + O^6-MeG dsDNA	2.38 ± 0.08	2.39 ± 0.10	2.27 ± 0.08
$(His)_6$-tagged C145A + O^6-MeG ssDNA	2.63 ± 0.22	2.70 ± 0.19	2.63 ± 0.10
$(His)_6$-tagged C145A + O^6-MeG dsDNA	4.76 ± 0.22	5.00 ± 0.34	4.17 ± 0.51
$(His)_6$-tagged C145S + O^6-MeG ssDNA	3.33 ± 0.21	3.57 ± 0.13	3.22 ± 0.24
$(His)_6$-tagged C145S + O^6-MeG dsDNA	5.36 ± 0.39	5.30 ± 0.39	5.60 ± 0.50

[a] Equilibrium binding reactions were carried out in 10 mM Tris (pH 7.6), 1 mM DTT, and 10 μg/mL bovine serum albumin at 21°C for 30 min. Since the repair reaction with O^6-methylguanine occurs rapidly, wild-type hAGT is unsuitable for specific binding assays. The active-site mutants used for this study, C145A and C145S, lack repair activity but retain full nonspecific binding affinity as shown in Table 1. [b] Monomer-equivalent formation constants, equal 1/[hAGT] at half-saturation of the 4:1 complex of hAGT with substrate 16-mer oligodeoxyribonucleotides. Error ranges represent the standard deviation for three replicate experiments.

Table 3: Total Repair Capacity of Zinc-Modulated hAGT[a]

	Repair Stoichiometry[b]		
	Zinc Preparation		
AGT protein	standard	supplemented	stripped
wild-type hAGT	0.992 ± 0.070	0.990 ± 0.040	0.972 ± 0.019
His-tagged wild-type hAGT	0.989 ± 0.030	0.991 ± 0.063	0.979 ± 0.081
His-tagged C5A	0.963 ± 0.018	0.968 ± 0.080	
His-tagged C24A	0.975 ± 0.090	0.980 ± 0.066	
His-tagged H29A	0.969 ± 0.038	0.973 ± 0.042	
His-tagged H85A	0.984 ± 0.070	0.983 ± 0.060	

[a] Data are calculated based upon known quantities of hAGT having been added to the reaction mixtures that were analyzed by quantitative reverse-phase HPLC for repaired DNA oligodeoxyribonucleotide product. Correlation of these measurements with the amount of protein added to each reaction mixture gives an estimate of the stoichiometry of repair. As the theoretical ratio of repaired DNA to hAGT is 1, the calculated repair stoichiometry is a measure of the fraction of repair active hAGT molecules in a given sample. [b] Moles of O^6-methylguanine repaired per mole of a given sample of hAGT protein. Error ranges represent the standard deviation for three replicate experiments.

site (*6*, *7*); however, it may not be part of the DNA-binding surface of the protein.

Effect of Zinc on Stoichiometry of hAGT-Mediated DNA Repair. Measurements of activity rate not only depend on the efficiency of each molecule in a given sample to effect alkyl transfer but also upon the total number of repair-active molecules within that sample. If the procedures employed to modulate zinc occupancy inactivated various populations of hAGT, measures of activity rate constants shown in Figures 3 and 4 would reflect sample manipulation rather than just the effects of zinc. Therefore, hAGT samples were assayed quantitatively for their total capacity to repair methylated oligodeoxyribonucleotide substrates. As a result of the irreversible stoichiometric alkyl transfer, which restores 5′-d(AACAGCCATATm^{6}GGCCC)-3′ to its nonalkylated cognate, tracking the disappearance of substrate and the formation of product after allowing repair of an excess substrate to proceed to completion allows determination of the number of active hAGT molecules. While rate constants for the proteins varied, the total repair capacities of the different samples were similar, and the high stoichiometries of repair (approaching the theoretical value of 1) suggest that they all contain relatively small fractions of inactive hAGT molecules (Table 3). Therefore, modulation of zinc occupancy by mutation and/or preparative means does not give rise to altered rates of repair activity by merely inactivating a significant portion of hAGT samples.

Effect of Zinc Content on hAGT Structure. Despite the preservation of repair capacity, the mutations and sample manipulations targeted at zinc occupancy might have induced radical structural perturbations in hAGT. Previous studies have shown that despite the lack of a known functional role for the protein's N-terminus, the stability of hAGT is highly sensitive to mutations in that region (*25*, *48*). Therefore, zinc-modulated and mutant hAGTs were analyzed by CD. Figure 6A depicts the far-UV spectrum of wild-type hAGT overlaid with spectra corresponding to zinc-supplemented and zinc-stripped preparations of the protein. Since these curves virtually superimpose, it can be inferred that modulation of zinc occupancy does not grossly affect the overall folded structure of hAGT. This result is consistent with the

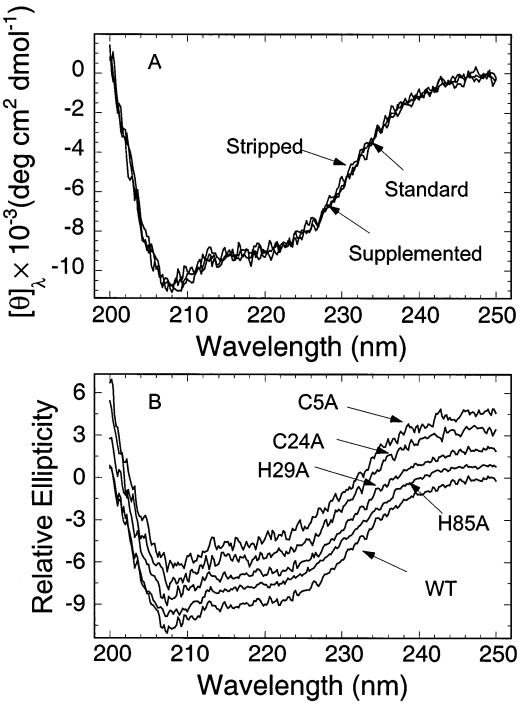

FIGURE 6: CD analysis of zinc-modulated hAGT proteins. Far-UV CD spectra of hAGT proteins were acquired to determine the secondary structural consequences of altering zinc occupancy. Tracings represent the average of three spectra acquired for each sample. Panel A: Spectra of standard, supplemented, and stripped hAGT (all at 25 °C) are overlaid to demonstrate the lack of change of CD with zinc occupancy. Experiments conducted at 37 °C (not shown) yielded similar results. Panel B: CD spectra of $(His)_6$-tagged wild-type hAGT and mutants in potential zinc binding residues, acquired at 37 °C. Tracings are offset with respect to ellipticity to allow comparison of spectra. Results were similar for zinc-supplemented samples of the same proteins and for scans taken at 25 °C (data not shown).

observation that the zinc-binding domain displays relatively similar conformations in both crystal structures despite the presence of bound metal in one and the absence of zinc in the other (*6*, *7*).

CD spectral analysis of zinc coordination residue mutants also revealed little effect on secondary structure. Standard preparations of wild-type hAGT, C5A, C24A, H29A, and H85A proteins all produced virtually identical ellipticity profiles as shown in offset plot in Figure 6B. Thus, manipulation of zinc content by chemical and mutational means does not alter the efficiency of alkyl transfer by inducing major changes in the secondary structure of hAGT.

Although CD revealed no significant structural changes as a function of zinc occupancy, fluorescence studies suggest that zinc binding results in altered protein conformation. The spectrum of zinc-supplemented wild-type hAGT demonstrates a small blue shift in emission maximum as compared to unsupplemented protein (result not shown). Zinc modulation may affect tertiary structure motifs in the vicinity of one or more of hAGT's four tryptophan residues (Trp65, Trp100, Trp167, and Trp191)

Effect of Zinc on hAGT Stability. The unfolding and refolding transitions of wild-type hAGT in the presence and absence of saturating $ZnCl_2$ were monitored fluorometrically (Figure 7). Although the equilibrium unfolding of hAGT does not fit a simple N ↔ U or N ↔ I ↔ U process, several qualitative conclusions can be reached. In zinc-supplemented

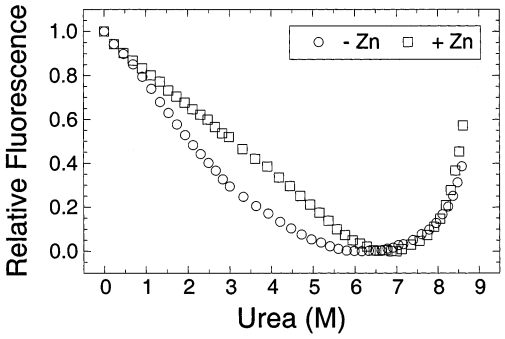

FIGURE 7: Fluorescence monitoring of unfolding transitions of wild-type hAGT in the presence and absence of zinc. The denaturing effects of urea on wild-type hAGT were tracked by fluorescence in the presence and absence of saturating $ZnCl_2$ (0.1 mM). Spectra were acquired for equilibrium solutions of wild-type hAGT (0.030 mg/mL) in 20 mM $NaPO_4$, 50 mM NaCl, and 1 mM DTT with concentrations of urea varied using an automated titrator as described in Materials and Methods. Relative fluorescence at 330 nm is plotted for both the standard (circles) and the zinc-supplemented (squares) preparations.

samples, the denaturation curve was shifted to the right, indicating that a higher urea concentration is necessary to disrupt the native fold. These data indicate that the protein is more resistant to denaturation in the presence of zinc, suggesting gain of stability with metal binding. Mutants of the zinc coordination residues were also studied using similar methods to investigate more directly the effect of occupancy of the metal binding site on structural stability (Figure 8). The mutation of Cys 24, in particular, virtually abolishes the zinc-induced stability enhancement that was apparent in experiments with wild-type hAGT (compare Figure 8B with Figure 7). Mutant C5A hAGT also exhibits a smaller increase in stability on zinc addition than the wild-type protein (Figure 8A). These results suggest that the denaturant resistant conformation adopted by hAGT in the presence of zinc may be mediated in large measure by metal binding of the two cysteines. While the mutants H29A and H85A only display minor deficits in zinc-mediated stability, neither showed the stability enhancement of wild-type hAGT with its intact zinc coordination sphere (Figure 8C,D).

DISCUSSION

Our studies provide compelling evidence that hAGT is a zinc metalloprotein and thus confirm the report based on the crystal structure (*6*). The simple gel-staining experiment shown in Figure 1 indicates that zinc forms stable complexes with hAGT since they survive prolonged electrophoresis in zinc-free buffer. Studies with ICP−MS confirm that zinc is a component of hAGT and that refolding of the protein in the presence of excess zinc leads to its incorporation into the protein structure. Lower levels of zinc in some recombinant hAGT preparations may be due to inadequate amounts of the metal in the culture to support the saturation of zinc binding sites in proteins expressed at very high levels from very strong promoters. The lack of zinc in the crystal structure of hAGT reported by Wibley et al. (*7*) may be explained in this way. Their structure of a C-terminal truncated protein was obtained using a N-terminally $(His)_6$-tagged sample. The zinc content at the native binding site may have been diminished by competition from the $(His)_6$-tag. Our studies using a C-terminally $(His)_6$-tagged protein show clearly that the presence of such a sequence increases the total zinc content, and it could also alter the distribution of zinc within the molecule in the nonsupplemented samples. It was reported recently that the C-terminally $(His)_6$-tagged protein has a slightly higher activity that the N-terminally $(His)_6$-tagged hAGT (*24*), and this protein was used in our studies. The proximity of the N-terminal $(His)_6$ addition to the native zinc binding site (particularly Cys5) may increase the potential competition for the limited zinc present in unsupplemented bacterial cultures. His-tagging is extremely convenient for the purification of hAGT and its mutants, but our results indicate that care should be taken to ensure that variations in zinc content caused by the tag do not influence experimental results with hAGT preparations. Using vectors that allow for the removal of the $(His)_6$-tag after purification would not solve this problem. Zinc-supplementation may be crucial to restore full occupancy to the critical site.

Our results also support the concept that zinc binding to the site in the hAGT N-terminal domain has a functional and stabilizing role. The functional role is indicated by the studies shown in Figures 3 and 4 where the rate of alkyl transfer from either O^6-methylguanine in DNA or O^6-benzylguanine was enhanced as a function of increased zinc content. This enhancement is clearly not due to the presence of zinc at the $(His)_6$-tag site since it was seen with nontagged protein as well.

A possible additional zinc-binding site in hAGT is indicated by the ICP−MS data (Figure 1B). Binding of transition metals to the surface of proteins is common as amino acids that can enter into such binding often occur in solvent-accessible regions. One such potential site is marked by Cys150. The C150A mutant hAGT has less zinc content than wild-type hAGT according to ICP−MS measurements. Considering the residue's proximity to the active site, zinc binding to the sulfur atom of Cys150 may interfere with the alkyl transfer reaction by electrostatic and/or steric effects. Binding of metal at that location on hAGT may explain some of the inhibitory properties of a wide variety of transition metal ions previously described (*10*, *11*). An interaction between Cys150 and zinc represents a plausible explanation for the global decrease in rates of alkyl transfer when $ZnCl_2$ was added to the assay medium with all proteins assayed in our experiments except C150A (Figures 3 and 4). However, the trend of activity rate constants varying in accordance with zinc occupancy at the N-terminal binding site persists whether zinc is present in assay solutions. These results resemble those found for murine adenosine deaminase, a key protein in immune system development, whose activity is enhanced by zinc binding at a particular tetrahedral coordination site but inhibited when zinc binds at certain surface residues (*49*).

The alkyl transfer rate enhancement by bound zinc appears to be independent of the protein's interaction with DNA since (a) changes in zinc occupancy do not influence binding affinities for alkylated and non alkylated DNAs and (b) the effect was seen with O^6-benzylguanine, which does not interact with the DNA binding domain. Although the zinc-binding site is located in the N-amino terminal domain, whereas the active site is located in the C-terminal domain and the difference between the zinc-possessing and the zinc-lacking crystal structures was small (*6*, *7*, *50*), zinc-binding has been suggested to alter the relative orientation of the

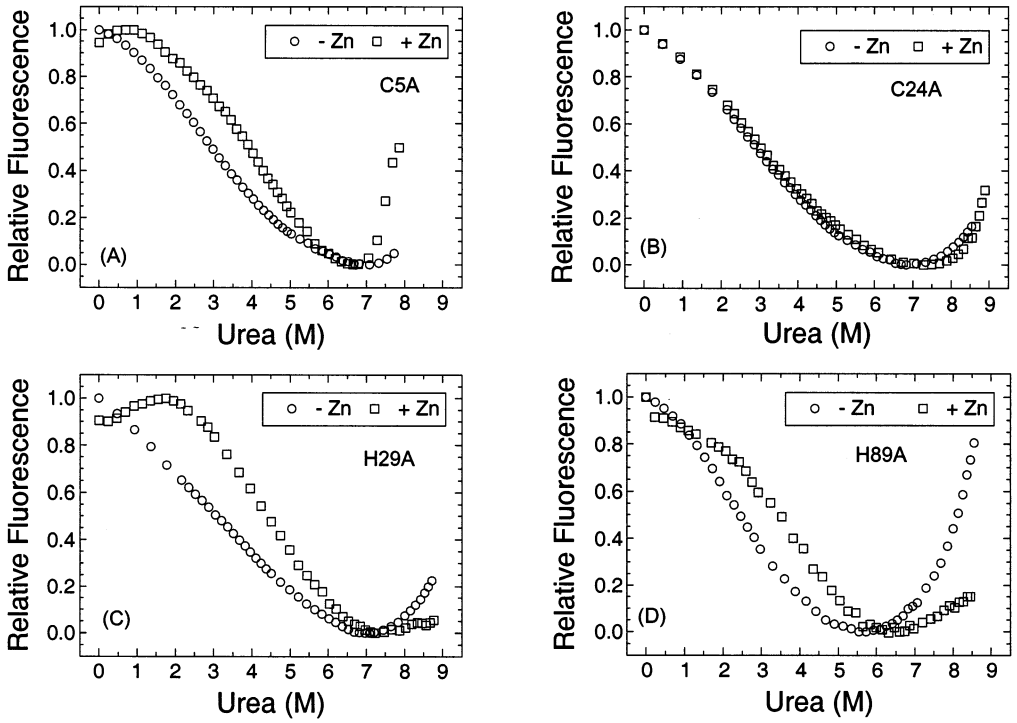

FIGURE 8: Fluorescence monitoring of unfolding transitions of mutant hAGT proteins in the presence and absence of zinc. The denaturing effects of urea on mutants of the zinc coordination sphere were tracked by fluorescence in the presence and absence of saturating $ZnCl_2$ (0.1 mM). Spectra were acquired for equilibrium solutions of hAGT proteins (0.023−0.030 mg/mL) in 20 mM $NaPO_4$, 50 mM NaCl, and 1 mM DTT with concentrations of urea varied using an automated titrator as described (cf. Materials and Methods). Relative fluorescence at 330 nm is plotted for both the standard (circles) and the zinc-supplemented samples (squares) for each of the four mutants. Unfolding transitions are shown for C5A (panel A), C24A (panel B), H29A (panel C), and H85A (panel D).

protein's two major domains (*6*, *50*). This change may affect the local positions of residues in the protein's active site that activate Cys145 to generate a thiolate anion for attack on the alkyl group of the substrate. Such changes may be too small to be detected in the CD analysis but could account for the minor changes in fluorescence observed as a function of zinc occupancy.

Zinc binding also improves the stability of hAGT and enhances the correct folding of the protein (Figures 7 and 8). This effect could contribute to the finding that recombinant hAGT expression was increased by supplementation of *E. coli* cultures with zinc (Figure 2). Cell growth at elevated zinc concentrations may raise the fraction of correctly folded hAGT molecules. Expression enhancement as a consequence of stability enhancement is also consistent with the results of denaturation/renaturation fluorescence experiments, which show evidence for a more stable structure in the presence of zinc. The occupancy of the N-terminal binding site by zinc may be essential to this stable conformation and the more efficient repair function that it performs.

It is probable that other mammalian AGT proteins are also zinc proteins since the residues involved in zinc coordination are maintained in these highly conserved proteins. However, these residues are absent in the amino acid sequences of microbial AGTs, and zinc was not found in the crystal structure of the *E. coli* Ada-C-terminal domain protein (*8*, *51*) or the protein from *Pyrococcus kodakaraensis* (*9*). It should be noted that even zinc-stripped hAGT is active in DNA repair, and the metal merely enhances reaction rate and protein stability. It is likely that other residues in the microbial AGTs provide the same steric function in activation of alkyl transfer and stability.

Another possibility that is worth experimental investigation is that the zinc-binding site in the N-terminal domain of hAGT may have evolved in response to the more complex subcellular environment of mammalian cells. Zinc occupancy may mediate the interaction of hAGT with other proteins, influencing its own regulation, or the regulation of other biochemical pathways. For example, zinc binding may change upon completion of the alkyl transfer reaction, resulting in a small conformational switch that targets hAGT for degradation. Since the ability of hAGT to form multiprotein complexes with DNA is diminished little following alkylation (J. J. Rasimas, unpublished observations), a signal other than dissociation from DNA must be necessary to target this stoichiometric repair protein for turnover. The decrease in hAGT stability we have observed in the absence of zinc indicates the potential validity of this hypothesis. It should be noted that despite lack of evidence for gross conformational switching with changes in metal occupancy, even subtle changes might reveal or obscure important binding sites on hAGT.

These findings regarding the influence of zinc on hAGT raise many questions about the metal's potential impact on alkylated DNA repair processes within cells. Obviously, zinc availability during translation and in the subcellular environments where the protein operates may affect hAGT function. The effects of metal concentration may not only impact the protection provided to normal cells by hAGT but also the degree to which tumor cells expressing the DNA repair protein show resistance to killing by alkylating agents (*52*). Furthermore, considering the dissimilarity of the binding site to previously described zinc coordination complexes and the lack of an obvious direct functional role for the metal ion,

zinc occupancy may determine a novel mode of biophysical regulation in hAGT. Although we have shown here that zinc binding has measurable in vitro consequences for structure and function of hAGT, it is in the milieu of the cell where the protein's interactions with other macromolecules may reveal a more detailed role for the metal. This underscores the importance of placing hAGT in the context of other biochemical processes by finding interacting partners for this seemingly solitary DNA repair protein. A more complete understanding of the role of the novel zinc site in hAGT is likely to depend on a complex network of biochemistry that extends well beyond the protein's own activity and structure.

ACKNOWLEDGMENT

We thank Dr. Greg Ferguson and Susan Lowery of Centre Analytical Labs in State College, PA for their expertise in performing metal quantitation analyses of AGT samples by ICP−MS. We also are grateful to Dr. Shaole Wu in the Chemistry Department of Penn State University whose preliminary ICP−MS measurements and technical assistance were vital to the success of this work. We thank Ms. Susi Sass-Kuhn for carrying out some protein purifications and Ms. Liping Liu for some plasmid constructions.

REFERENCES

1. Samson, L. (1992) *Mol. Microbiol. 6*, 825−831.
2. Sekiguchi, M., Nakabeppu, Y., Sakumi, K., and Tuzuki, T. (1996) *J. Cancer Res. Clin. Oncol. 122*, 199−206.
3. Pegg, A. E., Dolan, M. E., and Moschel, R. C. (1995) *Prog. Nucleic Acid Res. Mol. Biol. 51*, 167−223.
4. Pegg, A. E. (2000) *Mutation Res. 462*, 83−100.
5. Margison, G. P., and Santibáñez-Koref, M. F. (2002) *BioEssays 24*, 255−266.
6. Daniels, D. S., Mol, C. D., Arval, A. S., Kanugula, S., Pegg, A. E., and Tainer, J. A. (2000) *EMBO J. 19*, 1719−1730.
7. Wibley, J. E. A., Pegg, A. E., and Moody, P. C. E. (2000) *Nucleic Acid Res. 28*, 393−401.
8. Moore, M. H., Gulbus, J. M., Dodson, E. J., Demple, B., and Moody, P. C. E. (1994) *EMBO J. 13*, 1495−1501.
9. Hashimoto, H., Inoue, T., Nishioka, M., Fujiwara, S., Takagi, M., Imanaka, T., and Kai, Y. (1999) *J. Mol. Biol. 292*, 707−716.
10. Scicchitano, D., and Pegg, A. E. (1987) *Mutation Res. 192*, 207−210.
11. Bhattacharyya, D., Boulden, A. M., Foote, R. S., and Mitra, S. (1988) *Carcinogenesis 9*, 683−685.
12. O'Connor, T. R., Graves, R. J., de Murcia, G., Castaing, B., and Laval, J. (1993) *J. Biol. Chem. 268*, 9063−9070.
13. Buchko, G. W., Hess, N. J., Bandaru, V., Wallace, S. S., and Kennedy, M. A. (2000) *Biochemistry 39*, 12441−12449.
14. Morita, E. H., Ohkubo, T., Kuraoka, I., Shirakawa, M., Tanaka, K., and Morikawa, K. (1996) *Genes Cells 1*, 437−442.
15. Myers, L. C., Terranova, M. P., Ferentz, A. E., Wagner, G., and Verdine, G. L. (1993) *Science 261*, 1164−1167.
16. Myers, L. C., Jackow, F., and Verdine, G. L. (1995) *J. Biol. Chem. 270*, 6664−6670.
17. Pauly, G. T., Hughes, S. H., and Moschel, R. C. (1991) *Biochemistry 30*, 11700−11706.
18. Pauly, G. T., Powers, M., Pei, G. K., and Moschel, R. C. (1988) *Chem. Res. Toxicol. 1*, 391−397.
19. Pegg, A. E., Boosalis, M., Samson, L., Moschel, R. C., Byers, T. L., Swenn, K., and Dolan, M. E. (1993) *Biochemistry 32*, 11998−12006.
20. Ropson, I. J., and Dalessio, P. M. (1997) *Biochemistry 36*, 8594−8601.
21. McCloskey, D. E., and Pegg, A. E. (2003) *J. Biol. Chem.* (in press).
22. Kanugula, S., Goodtzova, K., and Pegg, A. E. (1998) *Biochem. J. 329*, 545−550.
23. Edara, S., Kanugula, S., Goodtzova, K., and Pegg, A. E. (1996) *Cancer Res. 56*, 5571−5575.
24. Liu, L., Xu-Welliver, M., and Pegg, A. E. (2001) *FASEB J. 15*, Abstract 519.
25. Crone, T. M., Goodtzova, K., Edara, S., and Pegg, A. E. (1994) *Cancer Res. 54*, 6221−6227.
26. Walker, J. M. (1994) *Methods Mol. Biol. 32*, 5−8.
27. Roy, R., Shiota, S., Kennel, S. J., Raha, R., von Wronski, M., Brent, T. P., and Mitra, S. (1995) *Carcinogenesis 16*, 405−411.
28. Fernandez-Patron, C., Castellanos-Serra, L., Hardy, E., Guerra, M., Estevez, E., Mehl, E., and Frank, R. (1998) *Electrophoresis 19*, 2398−2406.
29. Xu-Welliver, M., Kanugula, S., and Pegg, A. E. (1998) *Cancer Res. 58*, 1936−1945.
30. Pegg, A. E., Wiest, L., Mummert, C., Stine, L., Moschel, R. C., and Dolan, M. E. (1991) *Carcinogenesis 12*, 1679−1683.
31. Kanugula, S., Goodtzova, K., Edara, S., and Pegg, A. E. (1995) *Biochemistry 34*, 7113−7119.
32. Spratt, T. E., and Campbell, C. R. (1994) *Biochemistry 33*, 11364−11371.
33. Goodtzova, K., Kanugula, S., Edara, S., Pauly, G. T., Moschel, R. C., and Pegg, A. E. (1997) *J. Biol. Chem. 272*, 8332−8339.
34. Crone, T. M., and Pegg, A. E. (1993) *Cancer Res. 53*, 4750−4753.
35. Maxam, A. M., and Gilbert, W. (1977) *Proc. Natl. Acad. Sci. U.S.A. 74*, 560−565.
36. Fried, M. G., and Crothers, D. M. (1984) *J. Mol. Biol. 172*, 241−262.
37. Fried, M. G., Kanugula, S., Bromberg, J. L., and Pegg, A. E. (1996) *Biochemistry 35*, 15295−15301.
38. Pace, C. N. (1986) *Methods Enzymol. 131*, 266−280.
39. Gualfetti, P. J., Bilsel, O., and Matthews, C. R. (1999) *Protein Sci. 8*, 1623−1635.
40. Sacchettini, J. C., Gordon, J. I., and Banaszak, L. J. (1989) *Proc. Natl. Acad. Sci. U.S.A. 86*, 7736−7740.
41. Scapin, G., Gordon, J. I., and Sacchettini, J. C. (1992) *J. Biol. Chem. 267*, 4253−4269.
42. Hodsdon, M. E., Toner, J. J., and Cistola, D. P. (1995) *J. Biomol. NMR 6*, 198−210.
43. Hodsdon, M. E., and Cistola, D. P. (1997) *Biochemistry 36*, 2278−2290.
44. Navaratnam, S., Myles, G. M., Strange, R. W., and Sancar, A. (1989) *J. Biol. Chem. 264*, 16067−16071.
45. Yoneda, S., and Suzuki, K. T. (1997) *Biochem. Biophys. Res. Commun. 231*, 7−11.
46. Yoneda, S., and Suzuki, K. T. (1997) *Toxicol. Appl. Pharmacol. 143*, 274−280.
47. Leopold, I., and Fricke, B. (1997) *Anal. Biochem. 252*, 277−285.
48. Crone, T. M., Goodtzova, K., and Pegg, A. E. (1996) *Mutation Res. 363*, 15−25.
49. Cooper, B. F., Sideraki, V., Wilson, D. K., Dominguez, D. Y., Clark, S. W., Quiocho, F. A., and Rudolph, F. B. (1997) *Protein Sci. 6*, 1031−1037.
50. Daniels, D. S., and Tainer, J. A. (2000) *Mutation Res. 460*, 151−163.
51. Moody, P. C. E., and Moore, M. E. (1995) in *Novel Approaches in Anticancer Drug Design Molecular Modelling-New Treatment Strategies* (Zeller, W. J., D'Incalci, M., and Newell, D. R., Eds.) pp 16−24, Karger, Basel, New York.
52. Pegg, A. E., Xu-Welliver, M., and Loktionova, N. A. (2000) in *DNA alterations in cancer: genetic and epigenetic changes* (M. Ehrlich, E., Ed.) pp 471−488, Eaton Publishing, Natick, MA.

BI026970B